



Casein micelle formation as a calcium phosphate phase separation process: Preparation of artificial casein micelles through vacuum evaporation and membrane processes

Laurens J. Antuma^a, Maybritt Stadler^a, Vasil M. Garamus^b, Remko M. Boom^a, Julia K. Keppler^{a,*}

^a Laboratory of Food Process Engineering, Wageningen University & Research, Bornse Weiland 9, 6708 WG Wageningen, Netherlands

^b Helmholtz Zentrum Hereon, Max-Planck Str. 1, D-21502 Geesthacht, Germany

ARTICLE INFO

Keywords:

Cheese
Recombinant casein
Self-assembly
Forward osmosis
Reverse osmosis
Crystallisation

ABSTRACT

Industrial-scale production of artificial casein micelles (ACM) is required to produce dairy alternatives from recombinant casein. However, the currently common micelle preparation method of dropwise mixing casein and salt solutions is inefficient and may prove difficult to scale up. Here, we view casein micelle formation as a process driven by calcium phosphate phase separation in the presence of casein. On this basis, we developed novel routes to prepare ACM through vacuum evaporation, forward osmosis, or reverse osmosis. ACM prepared through these methods have similar properties and improved coagulation behaviour compared to those prepared through the currently common method and natural bovine casein micelles. The properties and functionality of the micelles depend on the preparation time and surface area available for micelle formation, with longer times and larger surfaces (i.e. lower fluxes) yielding smaller ACM that form firmer curds. These novel processes enable fast, efficient, and continuous production of ACM for application in future dairy alternatives.

Industrial relevance: Artificial casein micelles can be used as a building block in the production of animal-free milk and cheese based on precision fermentation. The herein described novel processes to prepare artificial casein micelles are based on vacuum evaporation, forward osmosis, and reverse osmosis, which are mild, resource-efficient, and easily scalable processes. The processes require a dilute feed stream (e.g. caseins after precision fermentation), provide an elegant way to minimise local differences in the concentration of caseins and ions during micelle production, and offer the opportunity to design continuous micelle formation processes. These are all advantages over the existing methods to prepare artificial casein micelles with regard to industrial application.

1. Introduction

Almost all biofluids in vertebrates, including blood, urine, saliva, and milk, are supersaturated with calcium phosphate; the primary constituent of bones and teeth (Holt & Carver, 2012). Calcium and phosphate in solution are prone to crystallisation and precipitation, the latter of which is prevented by the formation of nanocluster-type complexes stabilised by various compounds (Holt, Lenton, Nylander, Sørensen, & Teixeira, 2014). The formation of kidney stones in urine, for example, is impeded by crystallisation inhibitors for calcium oxalate and calcium phosphate (Fleisch, 1978). Similarly, caseins (a family of

phosphoproteins) prevent the pathological calcification of the mammary gland through the formation of hydrated colloidal structures termed casein micelles (Farrell, Malin, Brown, & Qi, 2006). In mammalian milk, these structures enable the safe transport of high amounts of calcium and phosphate to the neonate (Holt & Carver, 2012).

The assembly of caseins into casein micelles starts with the interaction between phosphoserine clusters of caseins and calcium phosphate nanoclusters (de Kruif & Holt, 2003; de Kruif, Huppertz, Urban, & Petukhov, 2012), the latter of which either forms on the phosphoserine clusters of caseins or free in solution followed by the rapid coating with casein (Holt, 1995; Holt & van Kemenade, 1989; Horne, 2020). Either

* Corresponding author at: PO Box 17, 6700 AA Wageningen, Netherlands.

E-mail addresses: laurens.antuma@wur.nl (L.J. Antuma), vasyl.haramus@hereon.de (V.M. Garamus), remko.boom@wur.nl (R.M. Boom), julia.keppler@wur.nl (J.K. Keppler).

<https://doi.org/10.1016/j.ifsset.2024.103582>

Received 6 December 2023; Received in revised form 11 January 2024; Accepted 15 January 2024

Available online 17 January 2024

1466-8564/© 2024 The Authors. Published by Elsevier Ltd. This is an open access article under the CC BY license (<http://creativecommons.org/licenses/by/4.0/>).

way, this interaction prevents the nanoclusters from further growth and delays their precipitation. Simultaneous casein self-association through various weak interactions then links additional caseins and other casein-stabilised nanoclusters to give rise to the supramolecular casein micelle structure.

Casein micelles can be prepared *in vitro* and these so-called artificial casein micelles (ACM) can play a crucial role in future food applications, for example as nanoencapsulants for numerous hydrophobic nutraceuticals (Tang, 2021) or as a building block in the production of animal-free alternatives to dairy products, such as milk and cheese (Hettinga & Bijl, 2022). Laboratory-scale processes to prepare ACM have been described in literature and were recently reviewed by Khan, Hemar, Li, Yang, and De Leon-Rodriguez (2023). In general, they include the controlled mixing of salt solutions containing high concentrations of calcium and phosphate, while simultaneously adding casein. The preparation of ACM allowed researchers to study the *ab initio* formation of casein micelles and assess the influence of different caseins and ionic species on their properties and stability. Thus, these procedures were not designed for industrial-scale production of ACM for application in food and may prove difficult to scale up. Therefore, it is pivotal to explore novel pathways to achieve the assembly of non-micellar caseins into casein micelles.

In this paper, we view casein micelle formation as a process driven by calcium phosphate phase separation in the presence of casein. Phase separation in the form of crystallisation usually occurs when the concentration exceeds the solubility of the components (i.e. when supersaturation is achieved), as the generation of nuclei, and eventually crystals, only occurs under nonequilibrium conditions (Erdemir, Lee, & Myerson, 2009; Lakerveld, Kuhn, Kramer, Jansens, & Grievink, 2010). Calcium phosphates, however, typically precipitate from solution following a pre-nucleation pathway in which first an amorphous phase, lacking the long-range order of crystalline material, is formed, which can mature into more crystalline phases in the absence of inhibitors through Ostwald ripening (Gebauer, Kellermeier, Gale, Bergström, & Cölfen, 2014; Lenton et al., 2016). Caseins strongly inhibit the crystallisation of calcium phosphate (van Kemenade & de Bruyn, 1989). Their binding affinity for amorphous calcium phosphate nanoclusters is so strong that complexes are created that are in a local free energy minimum with an activation free energy so high that the undesired maturation into crystalline particles is prevented (Lenton, Wang, Nylander, Teixeira, & Holt, 2020). In this view, it can be expected that inducing calcium phosphate phase separation in a solution in which caseins are present results in the formation of casein micelles. After all, the caseins would interact with the incipient calcium phosphate nanoclusters through their phosphoserine residues and subsequently self-assemble to form casein micelles.

Calcium phosphate phase separation can be attained by reducing the solubility of calcium phosphate through, for example, increasing the pH or temperature of the solution (McDowell, Gregory, & Brown, 1977; van Kemenade & de Bruyn, 1987). This technique has already been applied to study the interaction of β -casein peptides with calcium phosphate nanoclusters formed upon an increase in pH (Holt, Timmins, Errington, & Leaver, 1998; Holt, Wahlgren, & Drakenberg, 1996) and this method has been adapted to form artificial casein micelles (Raynes et al., 2023). Phase separation can also be achieved by increasing the concentration of calcium and phosphate ions in solution, which occurs during the aforementioned ACM preparation processes by carefully mixing solutions with calcium and phosphate ions. Alternatively, any form of water removal (e.g. evaporation or membrane permeation) from a dilute solution of calcium and phosphate would induce calcium phosphate phase separation. The crystallisation of calcium phosphates upon evaporation (Tanguy et al., 2016) and reverse osmosis (Paugam, Pouliot, Remondetto, Maris, & Brisson, 2022) has already been studied but it is yet to be explored whether these techniques can be employed to create ACM.

Therefore, we assess the validity of our hypothesis that casein micelle formation is essentially a calcium phosphate phase separation process in

the presence of caseins by inducing calcium phosphate phase separation in dilute solutions of salts and caseins. Thereby, we effectively concentrate the solutions until the approximate ion composition and protein concentration of bovine milk is reached. This is achieved through volume reduction by means of vacuum evaporation (VE), forward osmosis (FO), and reverse osmosis (RO). The resulting concentrates (hereinafter referred to as VE-ACM, FO-ACM, and RO-ACM, respectively) are then compared to ACM prepared according to Schmidt et al. (1977; hereinafter referred to as S-ACM).

2. Materials and methods

2.1. Materials

Bovine sodium caseinate (Lactonat EN, 89.8% protein, of which 33% α_s -caseins, 47% β -casein, 20% κ -casein, and 14.5 mg g⁻¹ sodium) was kindly donated by Lactoprot (Lactoprot Deutschland GmbH, Kaltkirchen, Germany). Bovine skim milk was purchased from a local supermarket. Calcium chloride (C1016), magnesium chloride (M8266), potassium phosphate monobasic (P5379), sodium phosphate dibasic (S7907), citric acid (C0759), potassium hydroxide (1.05033), sodium hydroxide (221465), potassium chloride (1.04936), potassium carbonate (1.04928), potassium sulfate (1.05153), trisodium citrate dihydrate (S4641), magnesium citrate tribasic nonahydrate (63067), hydrochloric acid (1.13386), nitric acid (1.00456), hydrogen peroxide (1.07209), sodium phosphate dibasic dihydrate (1.06580), citric acid monohydrate (1.00244), ethanol absolute (1.00983), guanidine hydrochloride (50950), L-dithiothreitol (D0632), and lactic acid solution (252476) were all purchased from Sigma-Aldrich (Merck KGaA, Darmstadt, Germany). Trifluoroacetic acid was purchased from Thermo Scientific (Thermo Fischer Scientific Inc., Waltham, MA, USA). Osmium tetroxide (19134), 50% glutaraldehyde solution (16316-10), and carbon adhesive tables (77825-12) were purchased from EMS (Electron Microscopy Sciences, Hatfield, PA, USA). Hydrochloric acid solution (7647-01-0) and acetonitrile ULC-MS (75-05-8) were purchased from Actu-All (Actu-All Chemicals B.V., Oss, Netherlands). Tripotassium citrate monohydrate (6100-05-6) was bought from VWR (VWR International bvba, Leuven, Belgium). Recombinantly produced chymosin (CHY-MAX Plus, batch no. 3634543) was obtained from Chr. Hansen Holding A/S (Hørsholm, Denmark). Ultrapure water (MilliQ system, Merck KGaA, Darmstadt, Germany) was used for all experiments.

2.2. Methods

2.2.1. Preparation of S-ACM

S-ACM were prepared according to Schmidt et al. (1977) with minor adjustments (hereinafter referred to as the Schmidt method). Sodium caseinate was dissolved in water to a casein concentration of 64.0 g L⁻¹ by stirring at 60 °C for 30 min and subsequently adjusted to pH 8.00 with 1 M NaOH. Three salt solutions were prepared: solution I contained 445 mM CaCl₂ and 75 mM MgCl₂ adjusted to pH 7.25 with 0.1 M HCl (approximately 18 mL L⁻¹), solution II contained 165 mM KH₂PO₄ and 165 mM Na₂HPO₄ adjusted to pH 7.25 with 1 M NaOH (approximately 200 mL L⁻¹), and solution III contained 135 mM citrate adjusted to pH 7.25 with 1 M KOH (approximately 460 mL L⁻¹). The caseinate solution (60 mL) and the salt solutions (10 mL each) were carefully pumped into a jacketed glass vessel at 37 °C containing a starting volume of 60 mL water in 60 min as described in Antuma et al. (2024). The solution was continuously and vigorously stirred using a magnetic stirrer. The pH decreased gradually from about 7.25 to 6.70 during preparation as a result of the release of protons during the formation of calcium phosphate nanoclusters (Visser & Jeurnink, 1997), which mimicked the gradual pH decrease during ACM preparation through volume reduction. The final pH was adjusted, if necessary, to pH 6.70 with a negligible volume of 1 M NaOH. The ACM were prepared in triplicate and stored at 4 °C for at least 12 h until analysis.

2.2.2. Preparation of feed solutions for concentration

Feed solutions contained 4.3 g L⁻¹ casein, 5.0 mM calcium, 3.7 mM phosphate, 0.8 mM magnesium, and 1.5 mM citrate. Although the solubility of pure calcium phosphate is generally estimated to fall in the range of a few mM or less (Christoffersen, Christoffersen, & Kibalczyk, 1990; van Kemenade & de Bruyn, 1987; Wang & Nancollas, 2008), its solubility is considerably increased (or its precipitation delayed) by the presence of phosphoproteins and other ions such as magnesium and citrate (Gelli, Ridi, & Baglioni, 2019; Johnsson & Nancollas, 1992; van Kemenade, 1988). In combination with the results of preliminary experiments shown in [Supplementary material A](#) and the absence of any visible precipitation in the feed solutions, we assumed the solutions to be undersaturated with respect to calcium phosphate. The solutions were prepared by first weighing the corresponding amounts of KH₂PO₄, citric acid, and MgCl₂ and dissolving them in water. The pH of this solution was then adjusted to about 7.0 with 1 M NaOH, after which the solution was added to the corresponding amount of sodium caseinate and stirred at 60 °C for 30 min. Next, the solution was left to cool to room temperature and CaCl₂ granules were then added to the solution while stirring. The pH of the solution was adjusted to 7.25 with 1 M NaOH. This pH value was determined in preliminary experiments to ensure that the pH after concentration would approximately be 6.70. In total, approximately 9 mL 1 M NaOH was used per litre of feed solution.

2.2.3. Preparation of VE-ACM

Exactly 900 mL of the feed solutions was carefully poured into 2 L prewetted evaporation flasks with indents (powder flask 514–75300-00, Heidolph Instruments GmbH & Co. KG, Schwabach, Germany) to ensure proper mixing of the solution. Vacuum evaporation was performed by using a batch-type rotary evaporator attached to a vacuum pump (RC 900 and SC 920 G, KNF Holding AG, Sursee, Switzerland) set at a pressure of 63 mbar, which corresponds to a boiling point of water of 37 °C (Wagner & Kretzschmar, 2008). The solutions were concentrated to 150 mL, corresponding to a concentration factor c_f of 6, by rotating the flasks at 30 rpm in a water bath set to 53 to 80 °C. This resulted in concentration times ranging from 105 to 41 min, respectively. If necessary, the pH of the ACM was adjusted to 6.70 with 1 M NaOH after evaporation. VE-ACM_{t=60 min} were prepared in triplicate and the rest in singlicate. The ACM were stored at 4 °C for at least 12 h until analysis.

2.2.4. Preparation of FO-ACM

Forward osmosis was carried out with an Aquaporin Inside® HFFO®2 hollow fibre forward osmosis module (Aquaporin A/S, Kongens Lyngby, Denmark) with an active membrane area of 2.3 m². Feed solutions were recircled through the lumen at a flow rate of 60 L h⁻¹ (inlet pressure of 0.4 bar) and draw solutions were passed through the shell side at 10 L h⁻¹ in single-pass mode by means of two gear pumps (VG1000 digit, Verder Deutschland GmbH, Haan, Germany) equipped with different pump heads (GB-P25.PVSA and GA-T23.JFSA, Micropump Inc., Vancouver, WA, USA). Feed and draw solutions were run in counter-current flow. Feed solutions with an initial volume of 6 L were concentrated to about 1 L ($c_f = 6$). The concentration time was controlled between 28 and 60 min by adapting the concentration of the draw solution from 0.20 to 0.12 M NaCl, respectively. Feed solutions were continuously stirred on a stirring plate and their temperature was controlled at 37 °C during concentration. If necessary, the pH of the ACM was adjusted to 6.70 with 1 M NaOH after concentration. FO-ACM_{t=60 min} were prepared in triplicate and the rest in singlicate. The ACM were stored at 4 °C for at least 12 h until analysis.

2.2.5. Preparation of RO-ACM

Reverse osmosis was conducted with a CUBE80-VA cross-flow laboratory filtration unit (SIMA-tec® GmbH, Schwalmatal, Germany) equipped with a membrane cell with an active membrane area of 85 cm². A flat sheet polyamide RO membrane (TRISEP® ACM2, MAN-N+HUMMEL Water & Fluid Solutions GmbH, Wiesbaden, Germany)

was installed in the membrane cell according to Ostertag, Krolitzki, Berensmeier, and Hinrichs (2023). Feed solutions with an initial volume of 3.6 L were pumped through the membrane cell at a rate of 30 L h⁻¹. A pressure of on average 33 bar was applied and the temperature was maintained at 37 °C by the temperature control unit. Filtrations were continued for about 22 h until 3 L permeate was collected ($c_f = 6$). To avoid microbial spoilage during an experiment, 0.02% (v/v) sodium azide was added to the feed solutions. If necessary, the pH of the ACM was adjusted to 6.70 with 1 M NaOH after concentration. RO-ACM were prepared in duplicate and stored at 4 °C for at least 12 h until analysis.

2.2.6. Ultracentrifugation and determination of apparent casein micelle hydration

ACM solutions were ultracentrifuged in duplicate and the apparent casein micelle hydration was determined through analysis of the moisture content of the pellet, both according to Antuma, Steiner, Garamus, Boom, and Keppler (2023).

2.2.7. Analysis of micellar casein composition

ACM solutions were diluted 5:1 and supernatants were diluted 2:1 in a buffer solution of 6 M guanidine hydrochloride, 20 mM dithiothreitol, and 5 mM sodium citrate and incubated for at least 1 h at room temperature before analysis (Bordin, Cordeiro Raposo, de la Calle, & Rodriguez, 2001). The total casein content and the casein content in the ultracentrifugal supernatants of samples were determined by reversed-phase high-performance liquid chromatography (RP-HPLC; Dionex UltiMate 3000 system, Thermo Fisher Scientific B.V., Breda, Netherlands) by using a VDSpher OptiBio Pur 300C4-SE column (VDS Optilab, Berlin, Germany) according to Schubert, Meric, Boom, Hinrichs, and Atamer (2018) with minor adjustments. The eluent composition during analysis is shown in [Table 1](#), where eluent A was composed of 1% (v/v) acetonitrile (ACN) and 0.1% (v/v) trifluoroacetic acid (TFA) in water and eluent B of 1% (v/v) water and 0.072% (v/v) TFA in ACN. Only linear gradients were used. The flow rate was set at 1.0 mL min⁻¹, the injection volume at 10 µL, the column temperature at 30 °C, and the detection wavelength at 214 nm. All analyses were performed in duplicate. Micellar casein was calculated as the difference between the total and supernatant casein.

2.2.8. Quantification of cations and anions

The concentration of cations (calcium, phosphorus, magnesium, sodium, and potassium) and anions (chloride, phosphate, and citrate) in ACM and their ultracentrifugal supernatants were determined as described in Antuma et al. (2024). Concentrations of ionic species in the supernatants were corrected with a correction factor calculated according to Pierre and Brule (1981). The micellar concentration of the ionic species was then calculated as the difference between the total concentration ([Table 2](#)) and the corrected supernatant concentration.

2.2.9. Small-angle X-ray scattering

Small-angle X-ray scattering (SAXS) measurements were performed at Helmholtz-Zentrum Hereon (Geesthacht, Germany) with a laboratory SAXS instrument (Xeuss 3.0, Xenocs SAS, Grenoble, France) according to Antuma et al. (2023).

Table 1
Eluent composition during RP-HPLC analysis.

Time (min)	Eluent A (%)	Eluent B (%)
0.0	72.0	28.0
21.5	62.4	37.6
22.5	62.4	37.6
26.0	54.0	46.0
28.0	0.0	100.0
29.0	0.0	100.0
30.0	72.0	28.0
35.0	72.0	28.0

Table 2

Total and expected concentrations of casein and calcium (Ca), inorganic phosphorus (P_i), magnesium (Mg), citrate (Cit), sodium (Na), potassium (K), and chloride (Cl) in the prepared samples.

Sample	Casein (g L ⁻¹)	Ca (mM)	P _i (mM)	Mg (mM)	Cit (mM)	Na (mM)	K (mM)	Cl (mM)
S-ACM _{t=60 min}	25.4 ± 0.3	29.0 ± 0.2	21.1 ± 0.3	4.6 ± 0.1	10.1 ± 0.1	55.7 ± 0.2	37.9 ± 0.3	68.0 ± 1.2
S-ACM (expected)	25.6	30.0	22.0	5.0	9.0	53.3	42.2	69.5
VE-ACM _{t=41 min}	25.1 ± 0.1	28.5 ± 0.5	19.7 ± 0.1	4.3 ± <0.1	8.2 ± 0.1	66.6 ± 0.9	20.8 ± 0.1	63.3 ± 0.1
VE-ACM _{t=46 min}	25.8 ± <0.1	28.9 ± 0.1	21.8 ± <0.1	4.4 ± <0.1	9.7 ± <0.1	68.4 ± 0.2	21.6 ± 0.3	68.3 ± 0.1
VE-ACM _{t=60 min}	24.8 ± 1.2	28.6 ± 0.2	21.5 ± 0.2	4.5 ± 0.1	9.3 ± 0.1	69.2 ± 0.5	22.4 ± 0.5	68.3 ± 1.3
VE-ACM _{t=80 min}	26.4 ± 0.5	28.3 ± <0.1	21.7 ± 0.4	4.5 ± <0.1	9.9 ± 0.2	70.0 ± 0.5	22.2 ± 0.1	69.2 ± 0.8
VE-ACM _{t=105 min}	26.5 ± 0.2	28.6 ± 0.4	21.2 ± <0.1	4.5 ± 0.1	9.6 ± <0.1	68.3 ± 1.2	22.5 ± 0.7	66.5 ± 0.1
FO-ACM _{t=28 min}	25.2 ± 0.4	23.4 ± 0.4	22.3 ± 0.1	4.3 ± 0.1	10.3 ± <0.1	122.7 ± 4.0	1.2 ± 0.1	103.5 ± 0.6
FO-ACM _{t=38 min}	28.1 ± 0.1	23.6 ± 0.3	23.3 ± 0.1	4.3 ± <0.1	10.6 ± <0.1	124.8 ± 0.7	0.9 ± 0.1	101.5 ± 0.4
FO-ACM _{t=60 min}	27.4 ± 2.7	25.6 ± 0.5	22.2 ± 2.4	4.5 ± 0.1	10.1 ± 1.0	121.7 ± 2.6	1.1 ± 0.6	102.5 ± 1.4
RO-ACM _{t=22 h}	23.0 ± 0.2	22.2 ± 0.2	18.3 ± 0.7	3.8 ± <0.1	8.5 ± 0.3	63.6 ± 1.0	15.9 ± 0.2	56.6 ± 2.0
VE/FO/RO-ACM (expected)	25.6	30.0	22.0	5.0	9.0	67.9	22.0	70.0

2.2.10. Scanning electron microscopy

Micellar morphology was visualised with scanning electron microscopy (SEM). One drop of sample was pipetted onto 12 mm poly-L-lysine glass slides (Corning Inc., Corning, NY, USA) and left to adhere for 30 min. Subsequently, the glass slides were washed twice with simulated milk ultrafiltrate (SMUF) prepared according to [Jenness and Koops \(1962\)](#). After removal of the SMUF, samples were fixed with 2.5% glutaraldehyde in 0.1 M phosphate/citrate buffer at pH 7.2 for 1 h. Afterwards, the fixative was removed and the glass slides were washed six times with SMUF. Samples were then fixed with a solution of 1% osmium tetroxide in SMUF for 1 h. The fixative was removed again and the slides were washed, dehydrated, critical point dried, sputter-coated, and mounted on specimen stubs according to [Antuma et al. \(2023\)](#). Images were taken at 100,000× magnification with a Magellan 400 microscope (FEI Company, Hillsboro, OR, USA) operating at a beam energy of 2 kV and a beam current of 13 pA.

2.2.11. Particle size analysis

Samples were diluted 50-fold in SMUF in square polystyrene cuvettes (67.742, Sarstedt AG & Co. KG, Nümbrecht, Germany), after which the size and polydispersity of the ACM were analysed with dynamic light scattering by using a Malvern Zetasizer Ultra (Malvern Panalytical Ltd., Worcestershire, UK). The device was equipped with a He–Ne laser with a wavelength of 633 nm. The refractive index of the dispersant was set at 1.33, its viscosity at 0.8872 mPa s, and the refractive index of the casein micelles at 1.57 ([Antuma et al., 2024](#)). Samples were first brought to room temperature and then equilibrated at 25 °C for 60 s inside the device before analysis. Measurements were carried out at 25 °C with a fixed scattering angle of 173°. Each sample was measured in duplicate and each replicate consisted of 5 sub-measurements, each of which consisted of a number of runs controlled by the ZS Xplorer software (version 2.3.1.4; minimum 25 runs). The harmonic intensity-weighted average hydrodynamic diameter (referred to as Z-average) and polydispersity index provided by the software were calculated by cumulant analysis using the general purpose model. Although this is a common method of analysing the size of casein micelles ([Bijl, van Valenberg, Huppertz, van Hooijdonk, & Bovenhuis, 2014](#); [Day, Raynes, Leis, Liu, & Williams, 2017](#); [Lenton et al., 2016](#)), it should be noted that the size of the measured particles was larger than the inverse scattering vector at the employed scattering angle, which yields an apparent Z-average rather than the true Z-average. Furthermore, dynamic light scattering should ideally be carried out over a range of scattering angles and in a concentration-dependent manner ([Zhuang, Ueda, Kulozik, & Gebhardt, 2018](#)). However, the gathered data still provide a good estimate of the relative differences in the sizes of the ACM between samples.

2.2.12. Rheological characterisation

ACM solutions were adjusted to pH 6.3 by means of acidification below 10 °C with an 8.5% lactic acid solution in water and left to equilibrate overnight at 4 °C. The pH was readjusted to 6.3 before

analysis. Subsequently, 0.04% (v/w) calcium chloride was added by means of a 4% (w/v) calcium chloride solution and the samples were heated to 30 °C while stirring. Samples were then renneted by adding 0.02% (v/w) chymosin and immediately transferred to a rheometer (MCR 302, Anton Paar, Graz, Austria) equipped with a double-gap device (DG26.7) to monitor the rennet-induced coagulation through oscillatory rheometry. A strain amplitude of 0.001 and a frequency of 1 Hz were applied at a fixed temperature of 30 °C (controlled by a Peltier element). The storage modulus G' of the samples was recorded for 60 min. Samples were analysed in duplicate.

2.2.13. Statistical data analysis

Statistical analysis of the data obtained from analyses on duplicate and triplicate samples was performed with OriginPro (version 2022, OriginLab Corporation, Northampton, MA, USA). Significance levels were assessed by one-way analysis of variance followed by Tukey's Honest Significant Difference post hoc test at a 95% confidence interval. Results are expressed as mean ± standard deviation of three independent triplicates. Results from analyses on samples prepared in singlicate are expressed as mean ± standard deviation of duplicate measurements (the latter of which equals the difference between the two values divided by $\sqrt{2}$).

3. Results

ACM solutions were prepared by using four different processes: 1) mixing casein and salt solutions according to an adaption of the Schmidt method and through volume reduction by means of 2) vacuum evaporation, 3) forward osmosis, and 4) reverse osmosis. Furthermore, the speed of micelle assembly was varied by varying the preparation time, which was 60 min for S-ACM, 41–105 min for VE-ACM, 28–60 min for FO-ACM and 22 h for RO-ACM. For ACM prepared through the volume reduction methods, a fixed concentration factor of 6 was applied based on preliminary experiments conducted with vacuum evaporation ([Supplementary material A](#)).

3.1. Scanning electron microscopy

The ACM were imaged with SEM to confirm the presence of micelles and enable visual comparison of ACM prepared with the different methods ([Fig. 1](#)). It can be seen that all four methods yielded mostly spherical particles in the size range of casein micelles and appeared to be approximately of similar size and size distribution. However, these images should be interpreted with care due to artefacts originating from invasive sample preparation ([McMahon & McManus, 1998](#)). With regard to this, further analysis of the particles in these pictures was not performed, also given the subjectivity of the analysis and dependence on image quality and contrast. Furthermore, it has been shown that analysis of particles in electron microscopy images results in a considerable

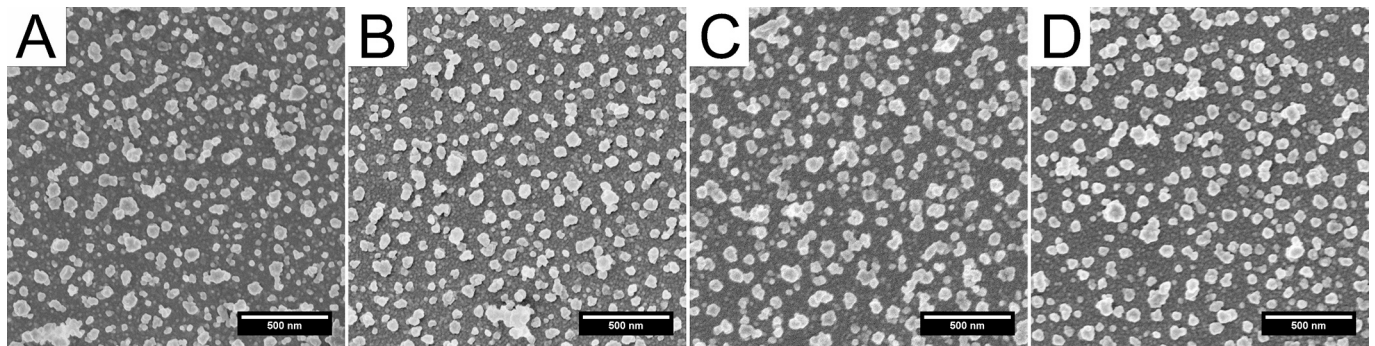


Fig. 1. SEM images of (A) S-ACM_{t=60 min}, (B) VE-ACM_{t=60 min}, (C) FO-ACM_{t=60 min}, and (D) RO-ACM_{t=22 h}. Scale bar = 500 nm.

underestimation of the particle size (Holt, Kimber, Brooker, & Prentice, 1978). Instead, the particles were further analysed with dynamic light scattering.

3.2. Sample compositions

We attempted to prepare ACM solutions with a similar composition with respect to the total concentrations of casein and ionic species. Table 2 shows the composition of the prepared ACM, which approximated the composition of bovine milk (Bijl, van Valenberg, Huppertz, & van Hooijdonk, 2013; Gaucheron, 2010). For S-ACM and VE-ACM, only the concentrations of sodium and chloride were significantly higher than those in bovine milk (18.0 and 25.6 mM, respectively; Bijl et al., 2013) due to the use of sodium caseinate, sodium hydroxide, and chloride salts for the preparation of ACM.

FO-ACM were slightly overconcentrated regarding the casein content, but most ion concentrations, and most notably those of calcium and potassium, were lower than the casein concentration suggested. The concentrations of sodium and chloride in these ACM, on the other hand, were considerably higher than in ACM prepared with other processes. This can be attributed to the diffusion of ions both from the feed to the draw solution (forward diffusion) and vice versa from the draw to the feed solution (reverse diffusion) during FO. Hancock and Cath (2009) found that forward and reverse diffusion of solutes depends on operating conditions, such as the composition and concentration of the draw solution and the cross-flow velocity. Monovalent ions, such as potassium, generally show higher forward diffusion than divalent ions, such as calcium (up to about 7 and 1.5 mmol m⁻² h⁻¹, respectively). For FO-ACM_{t=60 min}, we observed comparable values of, respectively, about 9 and 2 mmol m⁻² h⁻¹. These authors also reported reverse diffusion of ions from sodium chloride draw solutions generally in the range of 10 to 75 mmol m⁻² h⁻¹, which is comparable to the value of about 30 mmol m⁻² h⁻¹ that we found in our experiments for both sodium and chloride. Increased levels of sodium and chloride were previously found not to affect the composition and micelle properties of bovine casein micelles (Lazzaro et al., 2020; Schmidt et al., 1977; Schmidt & Koops, 1977) and we likewise expect limited effect of the increased levels of sodium and chloride on the properties of FO-ACM.

Finally, the RO-ACM appeared underconcentrated since the casein and ion concentrations were consistently lower than targeted (Table 2). In our RO experiments, the feed solution had an initial volume of 3.6 L and 3.0 L permeate was collected, in which no traces of casein or ions were found (data not shown). This means that the target concentration factor was reached and that the casein and ions were instead lost due to organic fouling and the formation of inorganic precipitates on the membrane (scaling). Nevertheless, ACM solutions with comparable compositions were obtained, which allowed for a relevant evaluation of the properties and functionality of the ACM.

3.3. Micelle properties

The size of the observed particles was characterised by using dynamic light scattering (Fig. 2). The diameter of S-ACM was measured at 156.3 ± 3.5 nm, which is considerably smaller than ACM prepared with the Schmidt method at an identical preparation time of 60 min (197.7 ± 4.1 nm) in our earlier work (Antuma et al., 2024). This can be explained by the higher proportion of κ-casein in the sodium caseinate used for the preparation of ACM in this study (20% as opposed to 17%) and the gradual pH decrease from 7.25 to 6.70 during ACM preparation. Nonetheless, the S-ACM were similar in diameter to natural bovine casein micelles, which generally range from 50 to 600 nm with an average size of about 150 nm (de Kruif, 1998) and were measured at 167.0 ± 0.8 nm with an almost identical method as in this work (Antuma et al., 2024). When an equal preparation time of 60 min was applied, the size of S-ACM (156.3 ± 3.5 nm) and VE-ACM (161.0 ± 7.6 nm) was not significantly different ($p = 0.73$). FO-ACM prepared within the same amount of time, however, were significantly ($p < 0.0001$) smaller at 121.9 ± 12.9 nm. The diameter of VE-ACM strongly depended on the preparation time, where increased preparation times yielded smaller micelles (Fig. 2A). This relation is reminiscent of the time-dependent assembly of ACM prepared with the Schmidt method as described in Antuma et al. (2024). In accordance with this trend, RO-ACM were significantly ($p < 0.0001$) smaller than S-ACM and VE-ACM due to the long preparation time. The size of FO-ACM did not depend on the preparation time.

Similarly, the polydispersity index (PDI) of VE-ACM decreased upon extending the preparation time (Fig. 2B), similar to the dependency of the PDI of S-ACM on the preparation time as observed by Antuma et al. (2024). The polydispersity of FO-ACM did not show a dependency on the preparation time and was significantly ($p < 0.0001$) lower than the 0.17 ± <0.01 for S-ACM. Thereby, the FO-ACM approximated the generally low polydispersity found for casein micelles in bovine milk (Antuma et al., 2024). VE-ACM prepared at an equal preparation time of 60 min had an even higher PDI of 0.35 ± 0.01, although this was not visually apparent from the SEM images (Fig. 1B).

Alternatively, the size and polydispersity of ACM prepared with the proposed methods based on volume reduction can be plotted against the flux of removed water during their preparation (Fig. 3). This flux takes into account both the preparation time as well as the volume of removed water and the surface area of evaporation or permeation. Fig. 3 shows that the fluxes were relatively low during the preparation of FO-ACM, whereas VE-ACM and RO-ACM were prepared with higher fluxes. The size and polydispersity of ACM increased with increasing flux and these properties were only considerably affected at fluxes larger than about 15 L m⁻² h⁻¹.

The fraction of the total amount of casein in the micellar phase was analysed by RP-HPLC (Table 3). In S-ACM, 90.6 ± 0.4% of the total amount of casein pelleted upon ultracentrifugation and was therefore assumed to represent the micellar phase. This is close to the level of

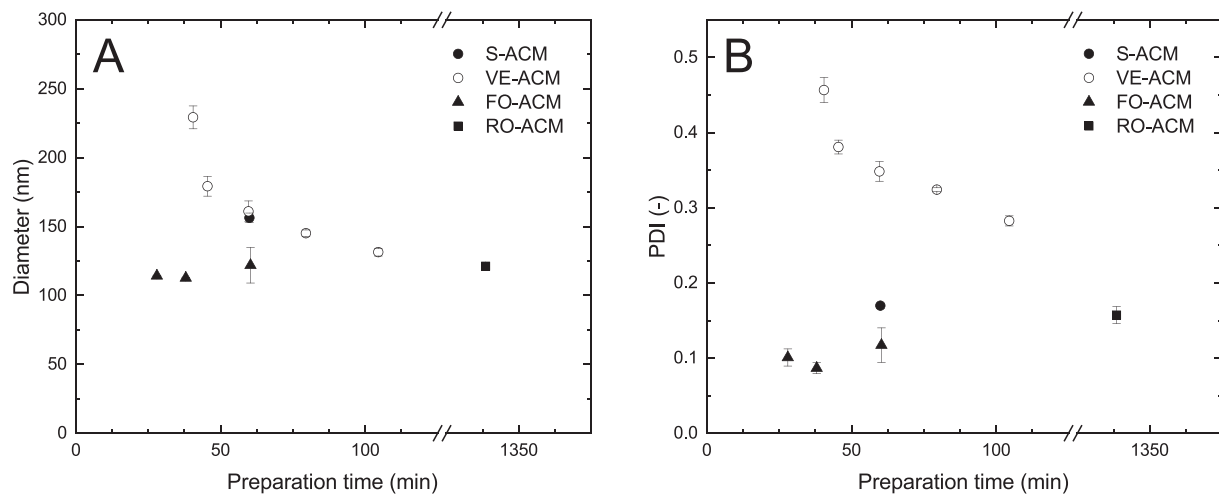


Fig. 2. (A) diameter and (B) polydispersity index (PDI) of ACM prepared with four different processes at various preparation times.

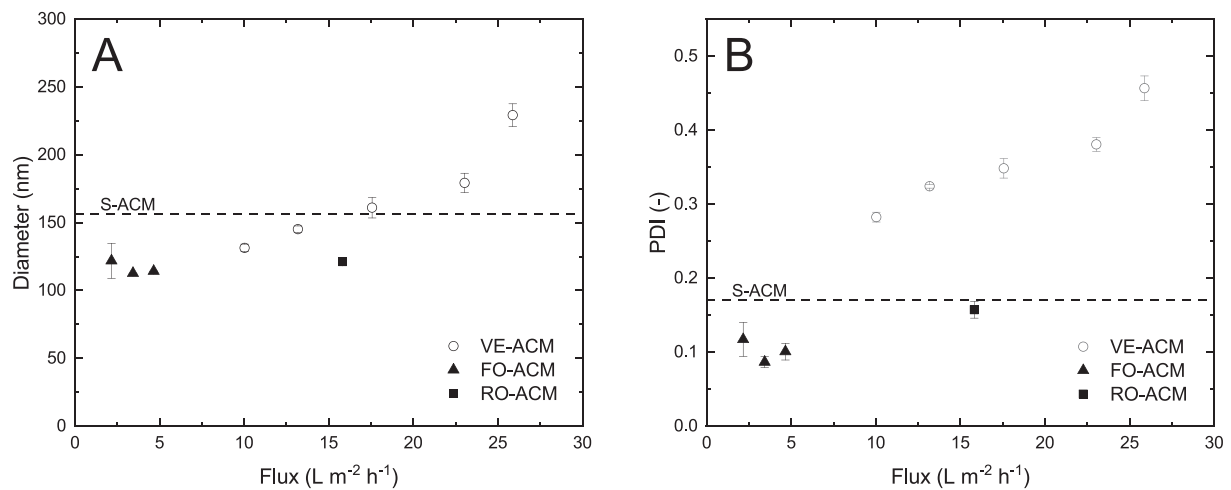


Fig. 3. (A) diameter and (B) polydispersity index (PDI) of ACM prepared with the proposed volume reduction methods plotted against the flux of removed water during their preparation. Due to the lack of a flux during their preparation, the size and PDI of S-ACM_{t=60 min} are represented by the dashed reference lines.

Table 3

Micellar casein as a proportion of the total amount of casein and the apparent hydration of the prepared ACM. Different superscript letters indicate significantly different results ($p < 0.0001$) within columns.

Sample	Micellar casein (%)	Apparent hydration (g water g ⁻¹ micellar casein)
S-ACM _{t=60 min}	90.6 ± 0.4 ^b	2.9 ± <0.1 ^b
VE-ACM _{t=41 min}	96.1 ± <0.1	2.8 ± <0.1
VE-ACM _{t=46 min}	95.8 ± 0.1	3.0 ± <0.1
VE-ACM _{t=60 min}	95.1 ± 0.5 ^a	2.9 ± 0.2 ^b
VE-ACM _{t=80 min}	95.8 ± 0.4	3.0 ± <0.1
VE-ACM _{t=105 min}	96.0 ± 0.2	2.9 ± <0.1
FO-ACM _{t=28 min}	91.4 ± <0.1	4.2 ± <0.1
FO-ACM _{t=38 min}	91.9 ± 0.1	4.4 ± 0.1
FO-ACM _{t=60 min}	95.1 ± 1.4 ^a	3.8 ± 0.4 ^a
RO-ACM _{t=22 h}	96.9 ± 1.6 ^a	3.1 ± <0.1 ^b

micellar casein in bovine skim milk (Antuma et al., 2024). VE-ACM_{t=60 min}, FO-ACM_{t=60 min}, and RO-ACM comprised a significantly ($p < 0.0001$) higher amount of casein at about 95–96% of the total casein, which did not show a relation with the preparation time. FO-ACM prepared at decreased preparation times contained lower amounts of micellar casein at about 91–92%. The apparent hydration of S-ACM, VE-

ACM, and RO-ACM was also similar at around 3 g water per g micellar casein (Table 3) and comparable to earlier findings (Antuma et al., 2024, 2023) and similar to the hydration of natural bovine casein micelles (Huppertz et al., 2017). FO-ACM were more hydrated and their hydration seemed to increase with shorter preparation times. The apparent hydration of VE-ACM did not depend on the preparation time.

The ACM were further characterised through analysis of the micellar concentration of ionic species (Table 4). S-ACM contained similar proportions of the total concentration of ionic species as observed by

Table 4

Proportion of the total concentration of ionic species present in the micellar phase of the ACM prepared with various methods.

Sample	Ca (%)	P _i (%)	Mg (%)	Cit (%)
S-ACM _{t=60 min}	71.5 ± 0.2	52.7 ± 1.0	38.6 ± 0.8	23.4 ± 1.6
VE-ACM _{t=41 min}	70.7 ± 0.6	50.0 ± 0.3	36.5 ± 0.1	12.3 ± 0.5
VE-ACM _{t=46 min}	70.1 ± 0.5	52.0 ± <0.1	36.9 ± 0.2	23.7 ± 0.1
VE-ACM _{t=60 min}	68.7 ± 1.0	48.1 ± 0.2	34.0 ± 0.8	17.4 ± 1.4
VE-ACM _{t=80 min}	69.6 ± 0.4	50.0 ± 0.1	35.1 ± 1.7	22.7 ± 0.3
VE-ACM _{t=105 min}	67.4 ± 0.3	46.1 ± 0.1	34.0 ± 2.0	20.0 ± 0.1
FO-ACM _{t=28 min}	66.8 ± 0.8	39.4 ± 0.2	33.1 ± 0.2	16.2 ± 0.4
FO-ACM _{t=38 min}	68.6 ± 0.3	41.7 ± 0.6	36.8 ± 0.8	19.0 ± 0.8
FO-ACM _{t=60 min}	68.7 ± 3.1	44.3 ± 3.2	35.9 ± 2.2	19.2 ± 2.7
RO-ACM _{t=22 h}	68.4 ± 0.4	47.3 ± 3.2	34.7 ± 0.7	17.3 ± 4.8

Antuma et al. (2023) and their mineralisation corresponded well to the mineralisation of natural bovine casein micelles (Bijl et al., 2013). VE-ACM, FO-ACM, and RO-ACM were mineralised to a similar extent, although these ACM seemed to contain a slightly lower proportion of the total concentration of ionic species than S-ACM. Little change in the mineralisation of the micelles was observed when they were prepared at various preparation times.

Next, SAXS measurements were carried out to compare the internal structure of the ACM. The overall shape of the obtained scattering profiles is typical for casein micelles (Fig. 4; Pedersen, Møller, Raak, & Corredig, 2022) with a strongly decreasing scattering intensity in a q -range from 0.005 to 0.03 \AA^{-1} , where the scattering from the interface of casein micelles follows the power law $I(q) \approx q^{-a}$ with a equal or close to 4. In the intermediate q -range, we observed the characteristic plateau where the scattering intensity decreases only slightly with increasing scattering angle. This region is commonly recognised to represent the substructure of casein micelles (i.e. calcium phosphate nanoclusters and protein inhomogeneities). At a larger q -values, a slope of about $q^{-2.2}$ was observed, which likely corresponds to the scattering of a semi-dilute solution of protein chains. A simple comparison of the scattering curves of the micelles prepared with different methods suggests only negligible changes in the substructure of the micelles.

Together, these results confirm that the ACM prepared with the four different methods all had a comparable substructure to natural bovine casein micelles and show that the ACM contained comparable concentrations of ionic species. Therefore, it is reasonable to conclude that calcium and phosphate were present in the form of nanoclusters of similar size as in natural bovine casein micelles in the prepared ACM.

3.4. Coagulation behaviour

The ACM were incubated with chymosin and the induced

coagulation was monitored over an hour with oscillatory rheometry (Fig. 5). After a lag phase of a few minutes, the storage modulus increased sharply as a result of the coagulation of the micelles. Within 60 min, S-ACM attained a storage modulus of 122.6 ± 1.0 Pa, similar to ACM prepared with the same method (Antuma et al., 2024) and commercial skim milk diluted to the same casein concentration with SMUF (117.6 ± 0.4 Pa) when coagulated under the same conditions. VE-ACM and FO-ACM with an equal preparation time attained significantly ($p \leq 0.01$) higher storage moduli of 141.6 ± 5.4 and 147.0 ± 12.2 Pa, respectively. RO-ACM yielded a lower storage modulus of 113.6 ± 0.1 Pa, relating to the lower concentrations of casein and calcium in these solutions due to membrane fouling (Table 2).

The preparation time also influenced the coagulation behaviour of VE-ACM (Fig. 6). The maximum attained storage modulus ranged from 117.3 ± 1.1 Pa for VE-ACM_{t=41 min} to 157.9 ± 0.2 Pa for VE-ACM_{t=105 min}. The coagulation behaviour of FO-ACM appeared relatively unaffected by the preparation time, although the onset of coagulation was delayed. This is likely related to the lower calcium concentration in these ACM, combined with increased concentrations of sodium and chloride. Both are known to prolong the rennet coagulation time (Lazzaro et al., 2020; Zoon, van Vliet, & Walstra, 1988, 1989). Nevertheless, no clear trend was observed in the attained maximum storage modulus of FO-ACM, which ranged from 132.3 ± 3.3 Pa for FO-ACM_{t=38 min} to 147.0 ± 12.2 Pa for FO-ACM_{t=60 min}. The observed differences were within experimental error and likely arose due to differences in the composition of these systems (Table 2) rather than the influence of the preparation time.

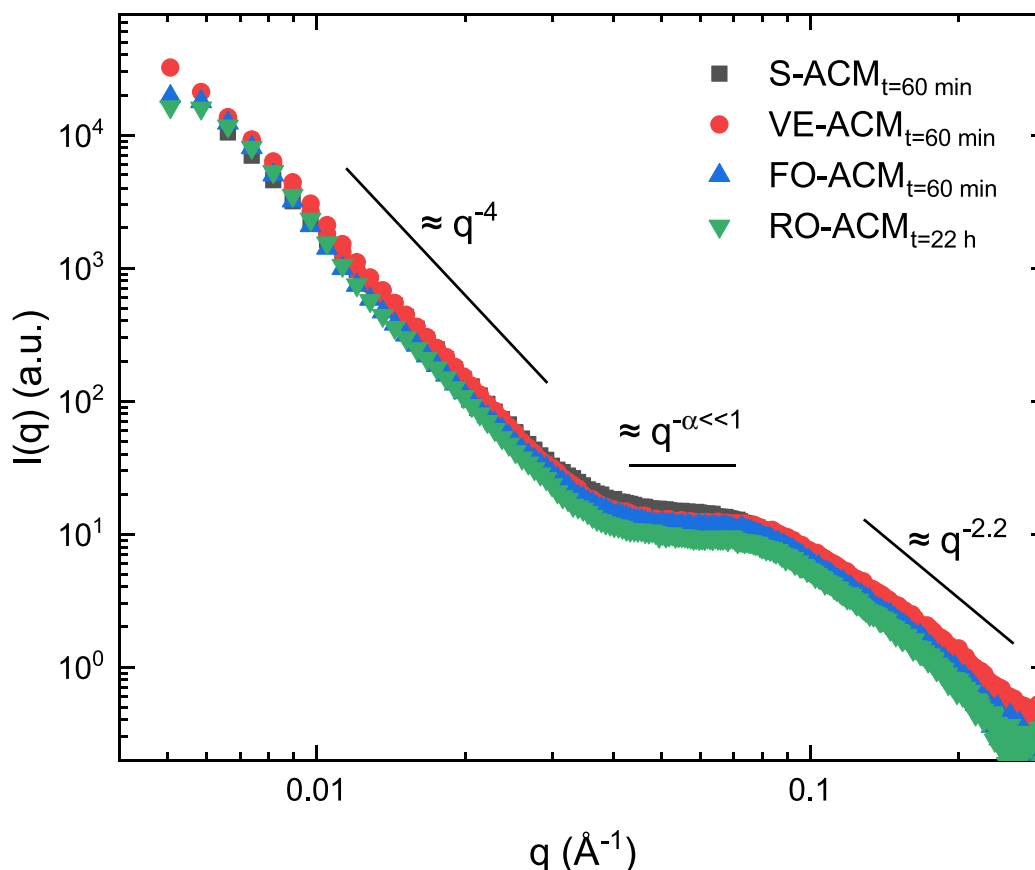


Fig. 4. Scattering intensities of S-ACM, VE-ACM, and FO-ACM with a preparation time of 60 min and RO-ACM with a preparation time of 22 h.

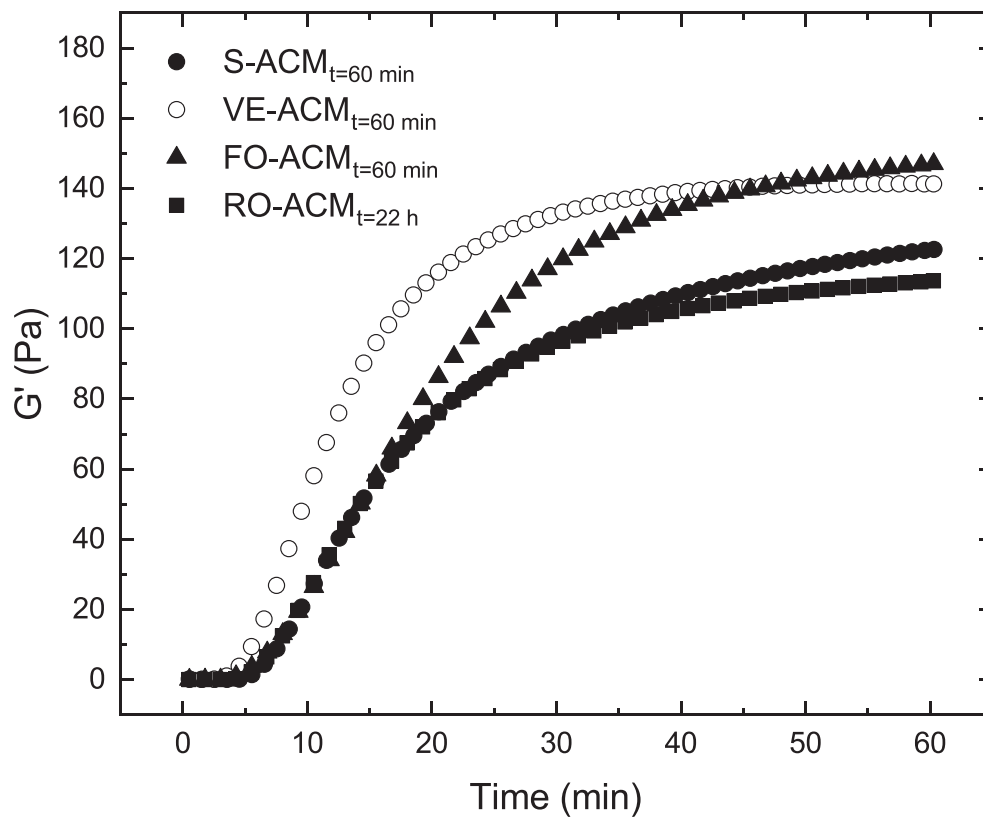


Fig. 5. Development of the storage modulus G' over time of ACM prepared with various methods incubated with chymosin.

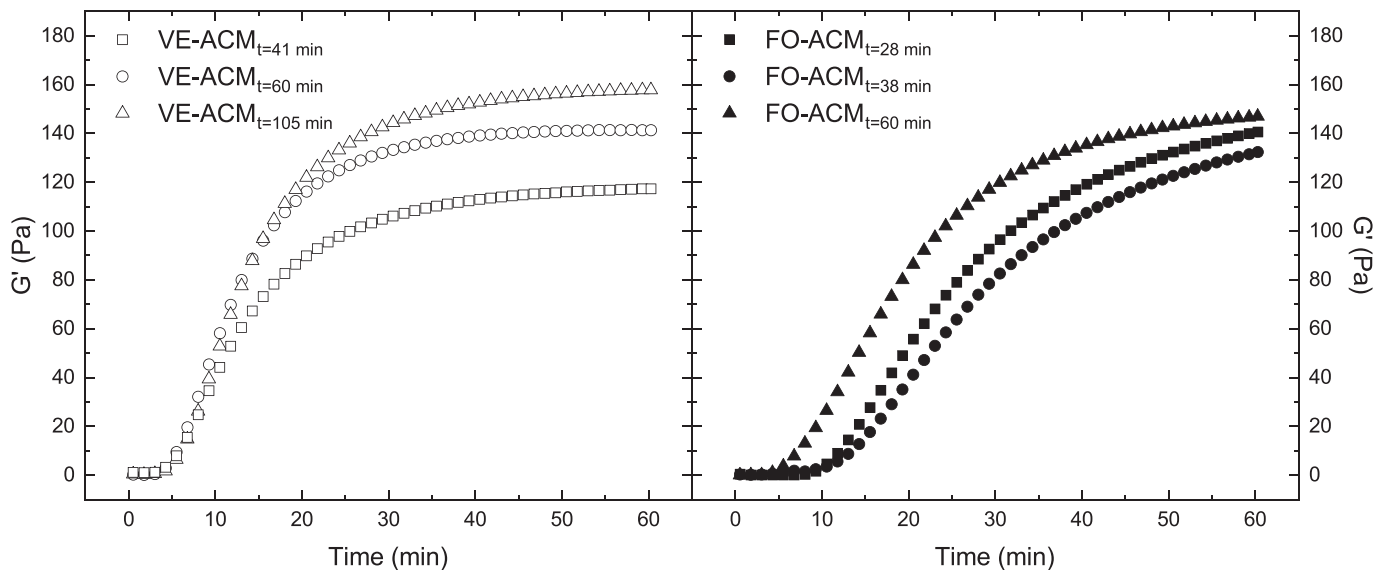


Fig. 6. Development of the storage modulus (G') of VE-ACM and FO-ACM with different preparation times over an hour of incubation with rennet.

4. Discussion

4.1. A novel method to prepare artificial casein micelles

Our results demonstrate that a controlled volume reduction (concentration) step was sufficient to induce casein micelle formation. Concentration of dilute solutions of calcium, phosphate, and casein through vacuum evaporation, forward osmosis, and reverse osmosis yielded spherical particles (Fig. 1) of a few hundred nanometres in diameter (Fig. 2A) with a similar internal structure (Fig. 4), which were

highly mineralised (Table 4) and hydrated (Table 3) and coagulated upon incubation with chymosin (Fig. 5). From these results, we deduce that these methods were successfully applied to prepare ACM. We envision that, during the volume reduction step, the solutions were gradually supersaturated with calcium and phosphate, which interacted to form insoluble calcium phosphate nanoclusters. Caseins either interacted with the preformed nanoclusters or acted as templates to initiate nanocluster growth, which neutralised the negatively-charged serine residues. This reduced the protein charge and allowed attractive interactions between caseins to dominate, which resulted in casein

self-assembly to yield the casein micelle structure. Although the commercial sodium caseinate of bovine origin that we used to create the ACM contained a lower proportion of α_s -caseins and a slightly higher proportion of κ -casein than typically found in bovine milk, we expect that the described interactions also occur when starting with a milk-like casein composition and that ACM will likewise be created upon applying a volume reduction step.

At an equal preparation time of 60 min, S-ACM and VE-ACM were of similar size (Fig. 2A) and hydration (Table 3). However, FO-ACM were significantly smaller and more hydrated than S-ACM and VE-ACM when prepared in equal preparation times. Since the proposed volume reduction methods all started with solutions of equal initial concentrations and yielded solutions of comparable final concentrations (Table 2), the only other variable during these experiments was the area of evaporation or permeation. Thus, the different micelle sizes are likely related to the large surface area available for permeation (i.e. the surface area over which micelle formation occurred) in our FO experiments (2.3 m²), which minimised local differences in the concentrations of calcium and phosphate. These concentration differences can be expected to have been larger during the preparation of ACM with the Schmidt method due to the nature of the process and with RO and VE due to the smaller area over which permeation and evaporation, and thus micelle formation, occurred (0.9 dm² for RO and on average approximately 4.3 dm² for VE; Supplementary material B). In Antuma et al. (2024), the magnitude of such local differences in the concentrations of calcium and phosphate was suggested to influence the micellar properties, where minimisation of local concentration differences by extending the preparation time yielded ACM of decreased size and polydispersity. Increasing the surface area over which micelle formation occurs would have a similar minimising effect on the local concentration differences as increasing the preparation time.

Thus, the properties of ACM prepared through volume reduction are better described by the flux of the removed water during their preparation, which takes into account both the surface area and preparation time, as well as the volume of the removed water (Fig. 3). Due to the larger surface area available for permeation, the flux during the preparation of FO-ACM was lower than that of VE-ACM and RO-ACM. This low flux translated to smaller local concentration differences during the preparation of FO-ACM, explaining their small size and low polydispersity. The size and polydispersity of RO-ACM were lower than expected given the flux during the RO experiments, which may be explained by lower concentrations of casein and ionic species in these ACM (Table 2) due to membrane fouling.

ACM prepared through the proposed volume reduction methods comprised a higher level of micellar casein of similar or increased hydration (Table 3) and, presumably as a result of that, generally formed firmer curds upon coagulation with rennet than micelles prepared with the Schmidt method (Fig. 5). Yet, RO-ACM exerted a similar curd firmness as S-ACM, presumably due to the lower casein and ion concentrations (Table 2). It is expected that RO-ACM would have yielded curds of similar firmness as VE-ACM and FO-ACM at equal sample compositions.

4.2. Effect of preparation rate on the properties of artificial casein micelles

In previous work, we showed that the properties and functionality of ACM prepared according to the Schmidt method were dependent on the applied preparation rate (Antuma et al., 2024). A negative logarithmic relation was found between the preparation time and the size and polydispersity of the micelles, with a characteristic time τ of about 18 min. At $t \gg \tau$, a steady state was reached where the size and polydispersity levelled off. In this study, VE-ACM also showed this dependency (Fig. 2). RO-ACM complied with this hypothesis since they were prepared over an extended time (22 h) and fitted in the trend with a decreased size of about 10 nm smaller. The size and PDI of FO-ACM,

however, did not depend on the preparation time (Fig. 2). Due to the previously discussed lower flux in these experiments (Fig. 3) and the concomitant smaller local concentration differences, it can be expected that the steady state shifted to shorter preparation times for FO-ACM. Thus, the size and PDI of these micelles would only be affected at preparation times shorter than assessed in this study. Assuming that these properties are indeed only significantly affected at fluxes higher than 15 L m⁻² h⁻¹ (Fig. 3), this suggests that the size and polydispersity of FO-ACM prepared with our experimental setup would only have been affected at preparation times shorter than 9 min. This conclusion is relevant in light of the potential scalability towards high production volumes.

By contrast, we here found that the size and polydispersity of VE-ACM already increased sharply at a considerably longer preparation time of around 40 min (Fig. 2), whereas they were previously found to increase for ACM prepared with the Schmidt method when the preparation time approached zero (Antuma et al., 2024). This can be explained by how the solution is concentrated during vacuum evaporation. Due to the applied rotation, a thin film is created on the inside wall of the evaporation flask, which increases the surface area over which evaporation occurs. Evaporation of water locally increases the concentration of the solutes more in this very thin film than it does in the bulk of the solution, where concentration differences are immediately compensated for by diffusion and the imposed flow. At the end of a rotation, the concentrated film comes into contact with the bulk solution and is effectively diluted by it, after which a new rotation starts. As a consequence, the formation of ACM was faster than the overall preparation time implies because the micelles are formed relatively fast and then diluted in the bulk solution. This caused the relation between the preparation time and the size and PDI of VE-ACM to shift to increased preparation times than previously established for ACM prepared with the Schmidt method.

In those instances where the preparation conditions influenced the properties of the ACM, this also resulted in differences in their coagulation behaviour (Fig. 6). The coagulation behaviour of VE-ACM prepared at shorter preparation times was impaired, presumably due to the increased size and polydispersity of the micelles (Fig. 2). It was previously shown that smaller casein micelles yield firmer curds upon coagulation (Niki & Arima, 1984) and ACM prepared with the Schmidt method have been found to show slower curd firming rates when prepared at shorter preparation times (Antuma et al., 2024). Since the properties of FO-ACM were hardly affected by the applied range of preparation times, their coagulation behaviour likewise remained relatively unaffected (Fig. 6).

4.3. Industrial relevance and outlook

To allow commercial production of animal-free foods with ACM from recombinant casein, both the expression of the casein and the preparation of ACM have to be realised on an industrial scale. In this section, we will focus on the industrial relevance of the proposed ACM preparation methods and place them in the context of the production of animal-free cheese from recombinant casein from the expression of the caseins to the coagulation of the ACM.

Vacuum evaporation, and especially forward osmosis and reverse osmosis, are mild, resource-efficient, and easily scalable processes. Vacuum evaporation is already used in the food industry for the production of tomato paste and in the dairy industry specifically for the pre-concentration of liquids during the production of dairy powders (Tanguy et al., 2016). Moreover, mainly reverse osmosis, but also forward osmosis, is commonly applied in the dairy industry, for example for the pre-concentration of milk to increase cheese yield (Cassano, Rastogi, & Basile, 2020). Therefore, the techniques and equipment to implement the proposed ACM preparation methods are readily available. In fact, preparing casein micelles artificially through volume reduction renders a pre-concentration step superfluous, since it provides the flexibility to

directly obtain solutions with the desired concentrations for cheesemaking.

Preparing ACM through volume reduction by means of vacuum evaporation, forward osmosis, or reverse osmosis has additional advantages over the existing method with regard to industrial application. Firstly, the production of recombinant proteins generally yields protein concentrations in the fermentation broth of several grams per litre or less, depending on the expression system (Demain & Vaishnav, 2009). Subsequent preparation of ACM with the Schmidt method would require drying the caseins after downstream processing or strongly concentrating the casein in solution, after which the caseins are diluted by mixing them with salt solutions and water during the preparation of the micelles. In contrast, the proposed ACM preparation methods based on concentration involve concentrating solutions with low initial casein concentrations of up to 4–5 g L⁻¹. Thus, caseins produced through precision fermentation can directly be assembled into micelles after downstream processing of the fermentation broth and the addition of salts, thereby avoiding a drying step (and its concomitant effects on protein quality) or a heavy concentration followed by a dilution of the proteins.

Furthermore, the proposed preparation processes based on volume reduction offer an elegant way of minimising local concentration differences during the preparation of ACM by increasing the surface area (i.e. by decreasing the flux). This allows for fast ACM preparation processes without affecting the properties and functionality of the micelles. In contrast, minimising local concentration differences during the preparation of ACM with the Schmidt method is more difficult due to the nature of the process and decreases the efficiency of the process (i.e. extended preparation times). In this study, we have estimated that our FO setup could prepare ACM in as short as 9 min without impairing the properties and functionality of the micelles, whereas Antuma et al. (2024) have shown that ACM prepared with the Schmidt method had increasingly poor functionalities when decreasing the preparation time from 60 to 15 min. In this regard, membrane processes generally lend more flexibility to increase the surface area than evaporation processes (Lakerveld et al., 2010).

Lastly, unlike the batch character of the Schmidt method, vacuum evaporation and membrane processes offer the potential for a continuous ACM preparation process. Dilute feed streams can continuously be pumped through an evaporator or membrane setup and concentrated until the desired concentrations are reached, which yields a continuous output stream containing the micellised casein. Other components, such as fats, can then be added to the micelle solution to optimise the formulation for the target food product. Next, this formulation can be acidified and/or renneted to coagulate the micelles and initiate the cheesemaking process. The condensate or permeate (pure water) originating from the concentration step and the ‘whey’ stream (comprising non-micellar casein, non-micellar ionic species, and part of the added components) originating from the coagulation step can be recycled to formulate new fermentation broth or to dilute the feed stream before

concentration. In the case of forward osmosis, the ‘permeate’ arises from the regeneration of the draw solution. Fig. 7 presents a simplified overview of the process.

There are also potential issues to consider when designing industrial-scale membrane processes to prepare ACM. For one, membrane fouling is a major issue in RO (Ahmed, Amin, & Mohamed, 2023), as we also observed in our experiments (Table 2). Compared to RO, fouling in FO is generally thought to be more reversible due to the different driving forces for osmosis (osmotic pressure and hydrostatic pressure, respectively), which is thought to result in a less compact fouling layer (Lee, Boo, Elimelech, & Hong, 2010; Xie, Lee, Nghiem, & Elimelech, 2015). Instead, our results show that reverse and forward diffusion of solutes need to be considered when designing an FO process for the preparation of ACM (Table 2). Future research could focus on the use of draw solutions of calcium or phosphate salts to enrich feed solutions in desired ions, thereby supporting micelle formation, rather than contaminating the solutions with undesired ions or drawing desired ions from them.

5. Conclusions

This study showed that casein micelle formation is driven by calcium phosphate phase separation in the presence of casein. Based on this principle, novel processes to prepare artificial casein micelles were proposed. These involve the concentration of dilute solutions of casein and salts by means of volume reduction through vacuum evaporation, forward osmosis, or reverse osmosis.

Artificial casein micelles prepared with these methods generally showed similar properties as those prepared with the hitherto prevailing method of Schmidt et al. (1977) at an equal preparation time. However, the proposed methods yielded increased levels of micellar casein and micelle hydration, which resulted in the formation of firmer curds upon rennet-induced coagulation. The properties and functionality of the micelles were affected by differences in the local concentrations of solutes during their preparation, which may be diminished by extending the preparation time or enlarging the surface area over which micelle formation occurs (i.e. decreasing the flux).

Thus, this study provides a first proof of concept of novel processes that allow the fast, efficient, and continuous production of artificial casein micelles for use in future food products.

CRedit authorship contribution statement

Laurens J. Antuma: Writing – original draft, Methodology, Investigation, Formal analysis, Conceptualization. **Maybritt Stadler:** Methodology, Investigation. **Vasil M. Garamus:** Writing – original draft, Methodology, Investigation, Formal analysis. **Remko M. Boom:** Writing – review & editing, Supervision, Funding acquisition, Conceptualization. **Julia K. Keppler:** Writing – review & editing, Supervision, Funding acquisition, Conceptualization.

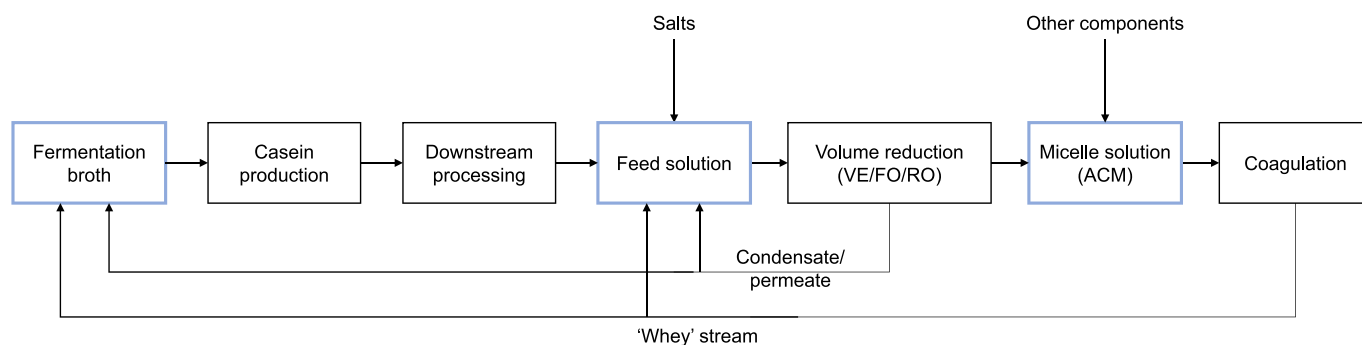


Fig. 7. Simplified overview of the production of animal-free cheese with recombinant casein from the production of recombinant casein to the coagulation of ACM, where the ACM are prepared through volume reduction by means of vacuum evaporation (VE), forward osmosis (FO) or reverse osmosis (RO).

Declaration of competing interest

The authors declare that they have no known competing financial interests or personal relationships that could have appeared to influence the work reported in this research. Three of the authors are cited as inventors on provisional patent application AU2023901874A that is based on the results presented in the present publication, but this application and all intellectual property rights to this work are held by Formo Bio GmbH (Berlin, Germany). The latter was part of the consortium that received funding from the European Union's Horizon 2020 research and innovation programme in which Wageningen University & Research participated. None of the authors have any pecuniary interest in the intellectual property rights nor do they benefit financially from this arrangement or from the commercial exploitation of this intellectual property.

Data availability

Data will be made available on request.

Acknowledgements

The work for this publication has been undertaken as part of the GOUDA project, which has received funding from the European Union's Horizon 2020 research and innovation programme through Eurostars (E! 114377). The authors would like to thank Jos Sewalt for translating our research ideas into practically feasible experiments and aiding in the design of those experiments. We thank Thomas Schubert of Formo GmbH and Nabil Chaib, Raphaela Klauß, and Melanie Rosenberger of the University of Hohenheim for realising and supporting the reverse osmosis experiments. Jörg Vogel and Yunfeng Li of Aquaporin A/S are kindly thanked for aiding in the design of the forward osmosis experiments and the interesting discussions of the results. Furthermore, we acknowledge Marcel Giesbers and Jelmer Vroom of the Wageningen Electron Microscopy Centre for their technical assistance with SEM imaging and Pieter Gremmen of the department of Environmental Technology for his help with the quantification of ions.

Appendix A. Supplementary data

Supplementary data to this article can be found online at <https://doi.org/10.1016/j.ifset.2024.103582>.

References

- Ahmed, M. A., Amin, S., & Mohamed, A. A. (2023). Fouling in reverse osmosis membranes: Monitoring, characterization, mitigation strategies and future directions. *Heliyon*, 9(4), Article e14908. <https://doi.org/10.1016/j.heliyon.2023.e14908>
- Antuma, L. J., Braitmaier, S. H., Garamus, V. M., Hinrichs, J., Boom, R. M., & Keppler, J. K. (2024). Engineering artificial casein micelles for future food: Preparation rate and coagulation properties. *Journal of Food Engineering*, 366, Article 111868. <https://doi.org/10.1016/j.jfoodeng.2023.111868>
- Antuma, L. J., Steiner, I., Garamus, V. M., Boom, R. M., & Keppler, J. K. (2023). Engineering artificial casein micelles for future food: Is casein phosphorylation necessary? *Food Research International*, 173, Article 113315. <https://doi.org/10.1016/j.foodres.2023.113315>
- Bijl, E., van Valenberg, H. J. F., Huppertz, T., & van Hooijdonk, A. C. M. (2013). Protein, casein, and micellar salts in milk: Current content and historical perspectives. *Journal of Dairy Science*, 96(9), 5455–5464. <https://doi.org/10.3168/jds.2012-6497>
- Bijl, E., van Valenberg, H. J. F., Huppertz, T., van Hooijdonk, A. C. M., & Bovenhuis, H. (2014). Phosphorylation of α_1 -casein is regulated by different genes. *Journal of Dairy Science*, 97(11), 7240–7246. <https://doi.org/10.3168/jds.2014-8061>
- Bordin, G., Cordeiro Raposo, F., de la Calle, B., & Rodriguez, A. R. (2001). Identification and quantification of major bovine milk proteins by liquid chromatography. *Journal of Chromatography A*, 928(1), 63–76. [https://doi.org/10.1016/S0021-9673\(01\)01097-4](https://doi.org/10.1016/S0021-9673(01)01097-4)
- Cassano, A., Rastogi, N. K., & Basile, A. (2020). Reverse osmosis in food processing. In A. Basile, A. Cassano, & N. K. Rastogi (Eds.), *Current trends and future developments on (bio-) membranes* (pp. 229–257). Elsevier. <https://doi.org/10.1016/B978-0-12-816777-9.00010-1>
- Christoffersen, M. R., Christoffersen, J., & Kibalczyk, W. (1990). Apparent solubilities of two amorphous calcium phosphates and of octacalcium phosphate in the temperature range 30–42°C. *Journal of Crystal Growth*, 106(2–3), 349–354. [https://doi.org/10.1016/0022-0248\(90\)90079-Z](https://doi.org/10.1016/0022-0248(90)90079-Z)
- Day, L., Raynes, J. K., Leis, A., Liu, L. H., & Williams, R. P. W. (2017). Probing the internal and external micelle structures of differently sized casein micelles from individual cows milk by dynamic light and small-angle X-ray scattering. *Food Hydrocolloids*, 69, 150–163. <https://doi.org/10.1016/j.foodhyd.2017.01.007>
- Demain, A. L., & Vaishnav, P. (2009). Production of recombinant proteins by microbes and higher organisms. *Biotechnology Advances*, 27(3), 297–306. <https://doi.org/10.1016/j.biotechadv.2009.01.008>
- Erdemir, D., Lee, A. Y., & Myerson, A. S. (2009). Nucleation of crystals from solution: Classical and two-step models. *Accounts of Chemical Research*, 42(5), 621–629. <https://doi.org/10.1021/ar800217x>
- Farrell, H. M., Malin, E. L., Brown, E. M., & Qi, P. X. (2006). Casein micelle structure: What can be learned from milk synthesis and structural biology? *Current Opinion in Colloid & Interface Science*, 11(2–3), 135–147. <https://doi.org/10.1016/j.cocis.2005.11.005>
- Fleisch, H. (1978). Inhibitors and promoters of stone formation. *Kidney International*, 13(5), 361–371. <https://doi.org/10.1038/ki.1978.54>
- Gaucheron, F. (2010). Analysing and improving the mineral content of milk. In M. W. Griffiths (Ed.), *Improving the safety and quality of milk* (pp. 207–228). Elsevier. <https://doi.org/10.1533/9781845699437.2.207>
- Gebauer, D., Kellermeyer, M., Gale, J. D., Bergström, L., & Cölfen, H. (2014). Pre-nucleation clusters as solute precursors in crystallisation. *Chemical Society Reviews*, 43(7), 2348–2371. <https://doi.org/10.1039/C3CS60451A>
- Gelli, R., Ridi, F., & Baglioni, P. (2019). The importance of being amorphous: Calcium and magnesium phosphates in the human body. *Advances in Colloid and Interface Science*, 269, 219–235. <https://doi.org/10.1016/j.cis.2019.04.011>
- Hancock, N. T., & Cath, T. Y. (2009). Solute coupled diffusion in osmotically driven membrane processes. *Environmental Science & Technology*, 43(17), 6769–6775. <https://doi.org/10.1021/es901133x>
- Hettinga, K., & Bijl, E. (2022). Can recombinant milk proteins replace those produced by animals? *Current Opinion in Biotechnology*, 75, Article 102690. <https://doi.org/10.1016/j.copbio.2022.102690>
- Holt, C. (1995). The biological function of casein?. In *HRI yearbook for 1994* (pp. 60–69). Hannah Research Institute.
- Holt, C., & Carver, J. A. (2012). Darwinian transformation of a 'scarcely nutritious fluid' into milk. *Journal of Evolutionary Biology*, 25(7), 1253–1263. <https://doi.org/10.1111/j.1420-9101.2012.02509.x>
- Holt, C., Kimber, A. M., Brooker, B., & Prentice, J. H. (1978). Measurements of the size of bovine casein micelles by means of electron microscopy and light scattering. *Journal of Colloid and Interface Science*, 65(3), 555–565. [https://doi.org/10.1016/0021-9797\(78\)90108-X](https://doi.org/10.1016/0021-9797(78)90108-X)
- Holt, C., Lenton, S., Nylander, T., Sørensen, E. S., & Teixeira, S. C. M. (2014). Mineralization of soft and hard tissues and the stability of biofluids. *Journal of Structural Biology*, 185(3), 383–396. <https://doi.org/10.1016/j.jsb.2013.11.009>
- Holt, C., Timmins, P. A., Errington, N., & Leaver, J. (1998). A core-shell model of calcium phosphate nanoclusters stabilized by beta-casein phosphopeptides, derived from sedimentation equilibrium and small-angle X-ray and neutron-scattering measurements. *European Journal of Biochemistry*, 252(1), 73–78. <https://doi.org/10.1046/j.1432-1327.1998.2520073.x>
- Holt, C., & van Kemenade, M. J. J. M. (1989). The interaction of phosphoproteins with calcium phosphate. In D. W. L. Hukins (Ed.), *Calcified tissue* (pp. 175–213). Macmillan Education UK. https://doi.org/10.1007/978-1-349-09868-2_8
- Holt, C., Wahlgren, M. N., & Drakenberg, T. (1996). Ability of a β -casein phosphopeptide to modulate the precipitation of calcium phosphate by forming amorphous dicalcium phosphate nanoclusters. *Biochemical Journal*, 314(3), 1035–1039. <https://doi.org/10.1042/bj3141035>
- Horne, D. S. (2020). Casein micelle structure and stability. In M. Boland, & H. Singh (Eds.), *Milk proteins: From expression to food* (3rd ed., pp. 213–250). Elsevier. <https://doi.org/10.1016/B978-0-12-815251-5.00006-2>
- Huppertz, T., Gazi, I., Luyten, H., Nieuwenhuijse, H., Altling, A., & Schokker, E. (2017). Hydration of casein micelles and caseinates: Implications for casein micelle structure. *International Dairy Journal*, 74, 1–11. <https://doi.org/10.1016/j.idairyj.2017.03.006>
- Jenness, R., & Koops, J. (1962). Preparation and properties of a salt solution which simulates milk ultrafiltrate. *Netherlands Milk and Dairy Journal*, 16, 153–164.
- Johnsson, M. S.-A., & Nancollas, G. H. (1992). The role of brushite and octacalcium phosphate in apatite formation. *Critical Reviews in Oral Biology & Medicine*, 3(1), 61–82. <https://doi.org/10.1177/10454411920030010601>
- van Kemenade, M. J. J. M. (1988). *Influence of casein on precipitation of calcium phosphates*. University of Utrecht.
- van Kemenade, M. J. J. M., & de Bruyn, P. L. (1987). A kinetic study of precipitation from supersaturated calcium phosphate solutions. *Journal of Colloid and Interface Science*, 118(2), 564–585. [https://doi.org/10.1016/0021-9797\(87\)90490-5](https://doi.org/10.1016/0021-9797(87)90490-5)
- van Kemenade, M. J. J. M., & de Bruyn, P. L. (1989). The influence of casein on the kinetics of hydroxyapatite precipitation. *Journal of Colloid and Interface Science*, 129(1), 1–14. [https://doi.org/10.1016/0021-9797\(89\)90411-6](https://doi.org/10.1016/0021-9797(89)90411-6)
- Khan, M. A., Hemar, Y., Li, J., Yang, Z., & De Leon-Rodriguez, L. M. (2023). Fabrication, characterization, and potential applications of re-assembled casein micelles. *Critical Reviews in Food Science and Nutrition*, 1–25. <https://doi.org/10.1080/10408398.2023.2193846>
- de Kruif, C. G. (1998). Supra-aggregates of casein micelles as a prelude to coagulation. *Journal of Dairy Science*, 81(11), 3019–3028. [https://doi.org/10.3168/jds.S0022-0302\(98\)75866-7](https://doi.org/10.3168/jds.S0022-0302(98)75866-7)

- de Kruijf, C. G., & Holt, C. (2003). Casein micelle structure, functions and interactions. In P. F. Fox, & P. L. H. McSweeney (Eds.), *Advanced dairy chemistry: Vol. 1. Proteins* (3rd ed., pp. 233–276). Springer US. https://doi.org/10.1007/978-1-4419-8602-3_5.
- de Kruijf, C. G., Huppertz, T., Urban, V. S., & Petukhov, A. V. (2012). Casein micelles and their internal structure. *Advances in Colloid and Interface Science*, 171–172, 36–52. <https://doi.org/10.1016/j.cis.2012.01.002>
- Lakerveld, R., Kuhn, J., Kramer, H. J. M., Jansens, P. J., & Grievink, J. (2010). Membrane assisted crystallization using reverse osmosis: Influence of solubility characteristics on experimental application and energy saving potential. *Chemical Engineering Science*, 65(9), 2689–2699. <https://doi.org/10.1016/j.ces.2010.01.002>
- Lazzaro, F., Bouchoux, A., Raynes, J., Williams, R., Ong, L., Hanssen, E., Lechevalier, V., Pezennec, S., Cho, H.-J., Logan, A., Gras, S., & Gaucheron, F. (2020). Tailoring the structure of casein micelles through a multifactorial approach to manipulate rennet coagulation properties. *Food Hydrocolloids*, 101, Article 105414. <https://doi.org/10.1016/j.foodhyd.2019.105414>
- Lee, S., Boo, C., Elimelech, M., & Hong, S. (2010). Comparison of fouling behavior in forward osmosis (FO) and reverse osmosis (RO). *Journal of Membrane Science*, 365(1–2), 34–39. <https://doi.org/10.1016/j.memsci.2010.08.036>
- Lenton, S., Nylander, T., Holt, C., Sawyer, L., Härtlein, M., Müller, H., & Teixeira, S. C. M. (2016). Structural studies of hydrated samples of amorphous calcium phosphate and phosphoprotein nanoclusters. *European Biophysics Journal*, 45(5), 405–412. <https://doi.org/10.1007/s00249-015-1109-7>
- Lenton, S., Wang, Q., Nylander, T., Teixeira, S., & Holt, C. (2020). Structural biology of calcium phosphate nanoclusters sequestered by phosphoproteins. *Crystals*, 10(9), 755. <https://doi.org/10.3390/cryst10090755>
- McDowell, H., Gregory, T. M., & Brown, W. E. (1977). Solubility of $\text{Ca}_5(\text{PO}_4)_3\text{OH}$ in the system $\text{Ca}(\text{OH})_2\text{-H}_3\text{PO}_4\text{-H}_2\text{O}$ at 5, 15, 25, and 37°C. *Journal of Research of the National Bureau of Standards Section A: Physics and Chemistry*, 81A(2–3), 273–281. <https://doi.org/10.6028/jres.081A.017>
- McMahon, D. J., & McManus, W. R. (1998). Rethinking casein micelle structure using electron microscopy. *Journal of Dairy Science*, 81(11), 2985–2993. [https://doi.org/10.3168/jds.S0022-0302\(98\)75862-X](https://doi.org/10.3168/jds.S0022-0302(98)75862-X)
- Niki, R., & Arima, S. (1984). Effects of size of casein micelle on firmness of rennet curd. *Japanese Journal of Zootechnical Science*, 55(6), 409–415.
- Ostertag, F., Krolitzki, E., Berensmeier, S., & Hinrichs, J. (2023). Protein valorisation from acid whey – Screening of various micro- and ultrafiltration membranes concerning the filtration performance. *International Dairy Journal*, 146, Article 105745. <https://doi.org/10.1016/j.idairyj.2023.105745>
- Paugam, N., Pouliot, Y., Remondetto, G., Maris, T., & Brisson, G. (2022). Impact of physicochemical changes in milk ultrafiltration permeate concentrated by reverse osmosis on calcium phosphate precipitation. *RSC Advances*, 12(39), 25217–25226. <https://doi.org/10.1039/D2RA02852B>
- Pedersen, J. S., Møller, T. L., Raak, N., & Corredig, M. (2022). A model on an absolute scale for the small-angle X-ray scattering from bovine casein micelles. *Soft Matter*, 18(45), 8613–8625. <https://doi.org/10.1039/D2SM00724J>
- Pierre, A., & Brule, G. (1981). Mineral and protein equilibria between the colloidal and soluble phases of milk at low temperature. *Journal of Dairy Research*, 48(3), 417–428. <https://doi.org/10.1017/S0022029900021890>
- Raynes, J. K., Mata, J., Wilde, K. L., Carver, J. A., Kelly, S. M., & Holt, C. (2023). Structure of biomimetic casein micelles: Critical tests of the hydrophobic colloid and multivalent-binding models using recombinant deuterated and phosphorylated β -casein. https://papers.ssrn.com/sol3/papers.cfm?abstract_id=4608131.
- Schmidt, D. G., & Koops, J. (1977). Properties of artificial casein micelles. 2. Stability towards ethanol, dialysis, pressure and heat in relation to casein composition. *Netherlands Milk and Dairy Journal*, 31(4), 342–351.
- Schmidt, D. G., Koops, J., & Westerbeek, D. (1977). Properties of artificial casein micelles. 1. Preparation, size distribution and composition. *Netherlands Milk and Dairy Journal*, 31(4), 328–341.
- Schubert, T., Meric, A., Boom, R. M., Hinrichs, J., & Atamer, Z. (2018). Application of a decanter centrifuge for casein fractionation on pilot scale: Effect of operational parameters on total solid, purity and yield in solid discharge. *International Dairy Journal*, 84, 6–14. <https://doi.org/10.1016/j.idairyj.2018.04.002>
- Tang, C. (2021). Strategies to utilize naturally occurring protein architectures as nanovehicles for hydrophobic nutraceuticals. *Food Hydrocolloids*, 112, Article 106344. <https://doi.org/10.1016/j.foodhyd.2020.106344>
- Tanguy, G., Siddique, F., Beaucher, E., Santellani, A.-C., Schuck, P., & Gaucheron, F. (2016). Calcium phosphate precipitation during concentration by vacuum evaporation of milk ultrafiltrate and microfiltrate. *LWT - Food Science and Technology*, 69, 554–562. <https://doi.org/10.1016/j.lwt.2016.02.023>
- Visser, J., & Jeurink, T. J. M. (1997). Fouling of heat exchangers in the dairy industry. *Experimental Thermal and Fluid Science*, 14(4), 407–424. [https://doi.org/10.1016/S0894-1777\(96\)00142-2](https://doi.org/10.1016/S0894-1777(96)00142-2)
- Tables of the properties of water and steam. In Wagner, W., & Kretzschmar, H.-J. (Eds.), *International steam tables* (2nd ed., (pp. 169–343). (2008) pp. 169–343). Springer Berlin, Heidelberg. https://doi.org/10.1007/978-3-540-74234-0_5.
- Wang, L., & Nancollas, G. H. (2008). Calcium orthophosphates: Crystallization and dissolution. *Chemical Reviews*, 108(11), 4628–4669. <https://doi.org/10.1021/cr0782574>
- Xie, M., Lee, J., Nghiem, L. D., & Elimelech, M. (2015). Role of pressure in organic fouling in forward osmosis and reverse osmosis. *Journal of Membrane Science*, 493, 748–754. <https://doi.org/10.1016/j.memsci.2015.07.033>
- Zhuang, Y., Ueda, I., Kulozik, U., & Gebhardt, R. (2018). Influence of β -lactoglobulin and calcium chloride on the molecular structure and interactions of casein micelles. *International Journal of Biological Macromolecules*, 107(Part A), 560–566. <https://doi.org/10.1016/j.ijbiomac.2017.09.021>
- Zoon, P., van Vliet, T., & Walstra, P. (1988). Rheological properties of rennet-induced skim milk gels. 3. The effect of calcium and phosphate. *Netherlands Milk and Dairy Journal*, 42, 295–312.
- Zoon, P., van Vliet, T., & Walstra, P. (1989). Rheological properties of rennet-induced skim milk gels. 4. The effect of pH and NaCl. *Netherlands Milk and Dairy Journal*, 43, 17–34.